ELSEVIER

Journal of Alloys and Compounds 262–263 (1997) 486–491

Journal of
ALLOYS
AND COMPOUNDS

Interactions in iron-based cermet systems

K. Aigner, W. Lengauer*, P. Ettmayer

Institute for Chemical Technology of Inorganic Materials, Vienna University of Technology, Getreidemarkt 9/161,
A-1060 Vienna, Austria

Abstract

The reactions occurring during sintering cermets were investigated at temperatures up to 1500°C. In the low temperature range (up to 500°C) physical reactions take place, in particular the vaporisation of residual milling agent and desorption of CO from the metal phase which remained from the production of the binder metal. From approximately 500°C up to the melting point of the binder the partial reduction of oxides from the surface of the carbides starts to remove carbon from the carbides and carbonitrides. This improves the wettability of the hard particles and leads to better densification. Below the temperature of formation of the liquid phase there is an intensive solid-state interaction between hard particles and binder metal. Due to the increased mobility of carbon the remaining surface oxides are reduced. This reaction is completed when the binder is molten, because at that time the oxygen from the hard particles' surface and binder is eaten up. In the third temperature range the liquid binder-phase starts to dissolve the hard particles, beginning at the grain boundaries. When the binder is saturated a solution–dissolution reaction takes place, reshaping and increasing the size of the particles. The porosity of Fe–Ti(C_xN_{1-x}) cermets after liquid phase sintering increases with the nitrogen content of the carbonitride. A comparison of the sintering behaviour of mixtures of group IV transition metals with iron shows an increase in porosity from Fe–TiC over Fe–ZrC to Fe–HfC. © 1997 Elsevier Science S.A.

Keywords: Titanium carbonitride; Zirconium carbonitride; Hafnium carbide; Sintering; Outgasing behaviour; Reactions

1. Introduction

Hardmetals and cermets are composite materials which have a combination of a hard but brittle hard phase with an elastic and tough binder leading to a composite having both hardness and toughness. These materials are used for cutting and drilling operations in the production of iron and steel parts. They have excellent properties but one drawback which is that nickel and cobalt are toxic heavy metals, their dust is especially harmful. Thus it is interesting to replace these metals by iron, which has the additional benefit of a low price and nearly unlimited resources. This work deals with the reactions of cermets with a binder content less than 35 wt.%, similar to cobalt-based cermets. In order to get a deeper insight into the sintering process, the different reactions between hard phase, binder phase and gas phase during the heating cycle were examined.

2. Experimental

The samples were prepared from powders of carbonyl iron (BASF), carbides, nitrides and carbonitrides (H.C. Starck). The composition and grain size of the starting powders are given in Table 1. All samples contain a fixed volume ratio of 3.5:1 of hard phase to binder phase. The constant volume ratio is important to compare the behaviour of hard particles

---

* Corresponding author. e-mail: wl@metec3.tuwien.ac.at

PII S0925-8388(97)00360-5

Table 1
Composition of starting powders

Powder	C (%)	N (%)	O (%)	Grain size (FSSS)
Iron	< 0.05	< 0.02	0.03	4–5 μm
TiC	19.57	0.074	0.0935	2.8 μm
ZrC	11.34	0.355	0.199	6.3 μm
HfC	6.06	0.278	0.033	6.3 μm
TiN	0.005	21.9	0.35	4.8 μm
Mo_2C	5.72	nm	0.199	1.5 μm
$TiC_{0.3}N_{0.7}$	6.6	14.3	0.45	5.0 μm
$TiC_{0.5}N_{0.5}$	9.7	11.1	0.27	3.3 μm
$TiC_{0.7}N_{0.3}$	13.3	6.8	0.2	4.1 μm

nm, not measured.

with different densities under equal conditions. After mixing, the samples were ball milled for 20 min under cyclohexane for better homogenisation and activation. Then the solvent was evaporated and the powder dried under vacuum. The oxygen content of the samples was analysed by means of vacuum hot extraction, the results are given in Table 2. The samples were cold pressed to pellets of 15 mm diameter in a hydraulic press at a pressure of 130 MPa.

The sintering experiments were carried out in an inductive furnace coupled with a quadrupole mass spectrometer (QMS 421, Balzers). The samples were heated in a molybdenum crucible on a bed of alumina. The temperature was measured by a thermocouple at the bottom of the crucible, a temperature controller allowed sintering at a constant heating rate. A constant carrier flow (argon or helium) was used for transporting the released gases of the samples to the mass spectrometer and allowed the on-line analysis of the gas phase during sintering. The concentrations of nitrogen and carbon monoxide were determined by a solution of a system of linear equations [1,2] based on the ion currents at mass 14 and 28, using the carrier as an internal reference.

The sintered bodies were cut, ground, polished and investigated by metallography and X-ray diffraction. In order to get additional information, samples were investigated by differential thermoanalysis (DTA 701, Bähr) and Dilatometry (801s, Bähr) to examine the shrinking behaviour.

3. Results and discussion

3.1. Interactions in Fe–TiC, Fe–ZrC, Fe–HfC

Mixtures of iron with titanium carbide, zirconium carbide and hafnium carbide were heated up to 1500°C at a heating ramp of 25°C/min. The outgasing behaviour of CO is shown in Fig. 1. All three curves exhibit a maximum at approximately 450°C, corresponding to the outgasing of pure carbonyl iron, by the desorption of unremoved CO from the production of the iron powder via the carbonyl process. The small peak at 300°C is caused by the removal of the milling agent. In the temperature range beginning at 500°C and increasing up to the melting point, different types of reaction can be seen. In the Fe–TiC mixture, the oxygen is almost completely removed within solid-state reactions at temperatures lower than 1150°C. Oxides on the surface of the titanium carbide are reduced according to the reaction:

$$x\mathrm{TiC} + \mathrm{TiO_2} => \mathrm{Ti}_{1+x}\mathrm{C}_{x-2} + 2\mathrm{CO}.$$

Within this process carbon diffuses into the oxide layer on the surface and gradually reduces the surface oxides. Sub-stoichiometic TiC_{1-x} is formed, which can be wetted more easily by binder. The oxides on the binder particles in direct contact with the carbide are also reduced.

The interaction between iron and TiC was examined closer using a solid state diffusion sample of compact iron in contact with TiC powder annealed for 196 h at 1100°C. A homogeneously distributed carbon content of 0.61 wt.% was found in the iron, showing carbon diffusion from the TiC into the binder metal, in agreement with the work of Popov [3]. Diffusion of titanium into the iron was not observed. The carbon

Table 2
Composition and oxygen content of powder mixtures

Sample	Sample weight (g)	Hard phase	Iron (wt.%)	Oxygen (wt.%)
Fe–TiC	4.3640	68.62 wt.% TiC	31.22	0.16
Fe–ZrC	6.8840	74.71 wt.% ZrC	24.98	0.31
Fe–HfC	12.2860	84.39 wt.% HfC	15.53	0.08
Fe–$TiC_{0.7}N_{0.3}$	4.3453	68.90 wt.% $TiC_{0.7}N_{0.3}$	30.93	0.17
Fe–$TiC_{0.5}N_{0.5}$	4.3030	69.18 wt.% $TiC_{0.5}N_{0.5}$	30.54	0.27
Fe–$TiC_{0.3}N_{0.7}$	4.2728	69.25 wt.% $TiC_{0.3}N_{0.7}$	30.49	0.26
Fe–TiN	4.3044	69.60 wt.% TiN	30.27	0.23

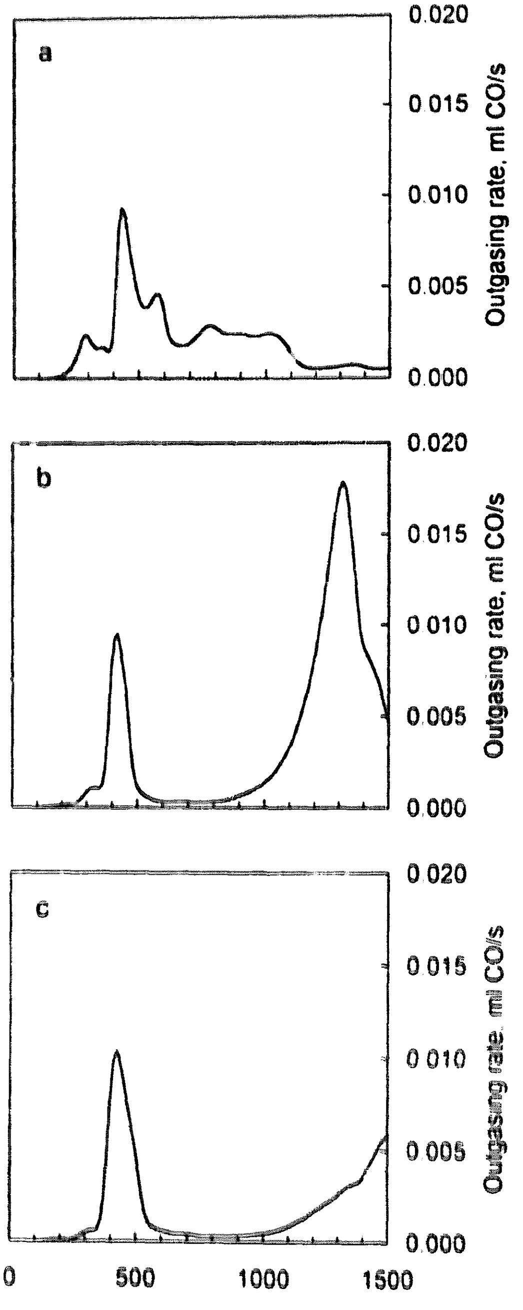

Fig. 1. Comparison of the CO formation of Fe–MeC composites (a: Fe–TiC; b: Fe–ZrC; and c: Fe–HfC).

diffusion into the binder allows the reduction of oxides at positions without direct contact of binder metal particles with the carbide. The oxygen removal is nearly completed within the solid state, therefore the CO production does not increase at temperatures higher than 1100°C (see Fig. 1). For liquid phase formation a temperature of 1300°C was found by DTA measurements, which is 50°C below the pseudobinary Fe–TiC eutectic [4]. The difference is caused by the increase of the carbon content in the iron during sintering. The α–γ transition of the binder in Fe–TiC samples was found to occur in the temperature interval of 730–800°C, corresponding to the work of Tofaute [5]. The decrease from 911°C (value for pure iron) is mainly caused by carbon diffusion in the iron, the interval is caused by a concentration gradient in the binder.

When the temperature of liquid phase formation is reached a solution–dissolution process starts resulting in an increase of the grain size of the hard particles, liquid phase sintering of the Fe–TiC mixture at 1400°C for 4 h doubles the grain size relative to the starting powder (Fig. 2).

In order to examine the relationship between oxygen localisation and CO formation closer, Fe–TiC samples containing additional oxygen were examined. The outgasing behaviour of a mixture of iron powder with an oxygen content of 0.4% (obtained by oxidising the iron powder for 7 days at 150°C in air) with TiC is shown in Fig. 3. The CO peak coming from the iron is increased and its position is shifted slightly towards higher temperatures (490°C). Additionally, an increased CO evaluation above the temperature of liquid phase formation can be observed.

Oxygen in the carbide phase (Fig. 4), supplied as oxycarbide in a Fe–$Ti(O_{0.1}C_{0.9})$ mixture leads to an increase in the CO formation at $T > 700$°C, due to the removal of oxides on the surface of the oxycarbide by solid state reaction. The CO formation decreases when the liquid phase appears, but is increased again when the dissolution in the liquid phase starts. The reduced wettability of the oxycarbide in comparison to the pure carbide and the high quantity of released CO press the binder out of the sample, which stays porous.

In the iron–zirconium carbide mixtures the oxygen removal starts at 800°C having a maximum at the temperature of the γ–δ transition in the Fe–ZrC system (1370°C) [6]. The main part of the oxygen is removed in a solid-state reaction. The amount of evolved CO is relatively high in comparison to the mixture containing TiC and HfC due to the higher oxygen content of the Fe–ZrC mixture (0.3 wt.%). When the surface oxygen of the carbide and the oxygen of the iron are used up, a decrease in the CO formation is observed.

The outgasing of Fe–HfC shows an increase of the CO production beginning at approximately 950°C, caused by the reduction of surface oxides. The principle behaviour of the CO production curves in Fe–ZrC and Fe–HfC samples, i.e. increasing of CO rate upon approaching the temperature of occurrence of the liquid phase (CO maximum) is similar to that of Fe–Ti(O,C). When the temperature of eutectic melting [6] in the Fe–HfC system is reached (1490°C) the CO forming is not finished, due to a solution–dissolu-

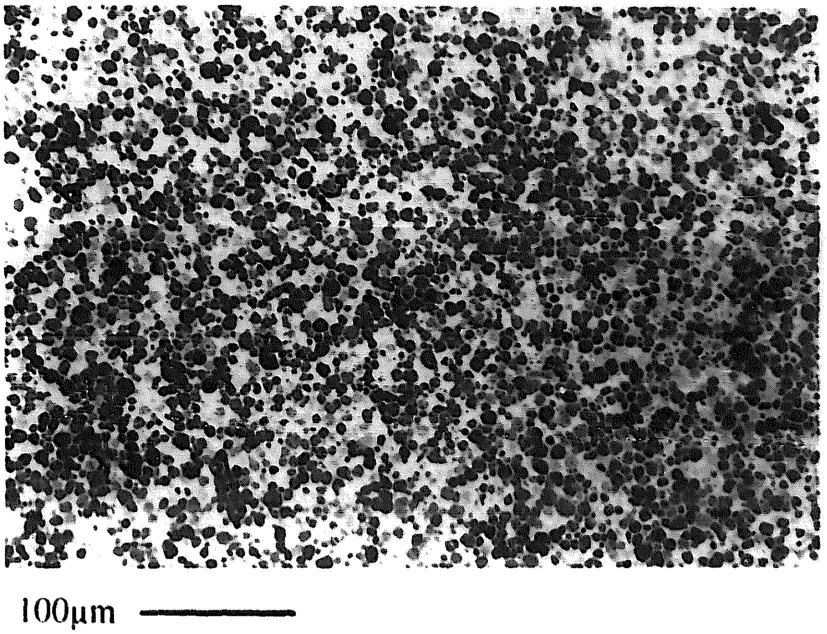

Fig. 2. Microstructure of a Fe-TiC composite after 4 h annealing at 1400°C light grey: Fe, dark particles: TiC (in rounded shape).

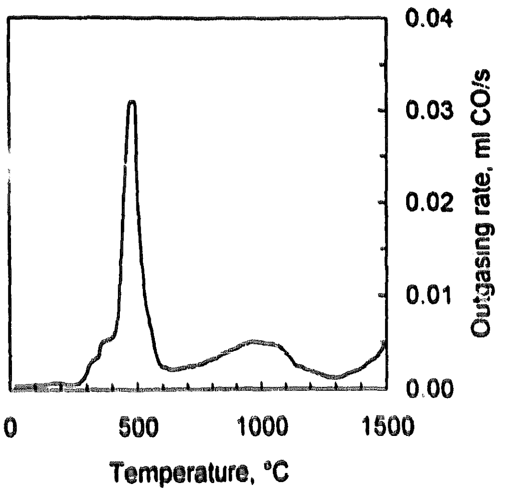

Fig. 3. CO formation of a Fe(0.4%O)-TiC composite.

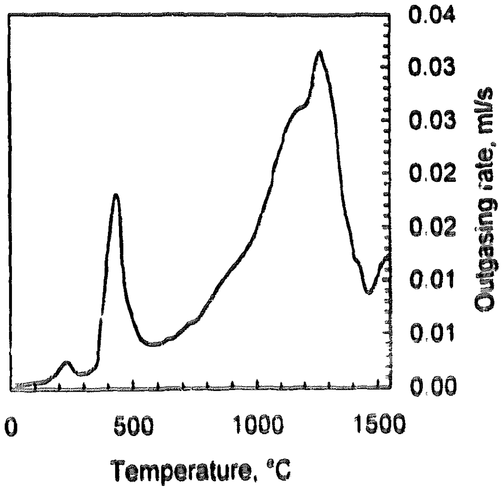

Fig. 4. CO formation of a Fe-Ti($O_{0.1}C_{0.9}$) composite. At $T \approx 450°C$, outgasing from iron; at $T \geq 700°C$ solid-state CO removal.

tion process, bringing oxygen from the carbide grains in contact with the carbon containing iron melt.

The starting temperature of the oxide reduction in the iron-carbide systems (Fe-TiC: 650°C, Fe-ZrC: 850°C and Fe-HfC: 950°C) goes parallel with the stability of the oxides, TiO_2 is less stable than ZrO_2 which in turn is less stable than HfO_2.

Metallographic investigations showed that iron-titanium carbide mixtures sintered relatively dense (Fig. 5), the porosity increases from Fe-TiC over Fe-ZrC to Fe-HfC.

3.2. Interaction between Fe and Ti (C,N)

The outgasing behaviour of mixtures of iron with $TiC_{0.7}N_{0.3}$, $TiC_{0.5}N_{0.5}$, $TiC_{0.3}N_{0.7}$ and TiN in the temperature range between 1000 and 1550°C is shown in Fig. 6a-d. The outgasing curves of the carbonitrides $TiC_{0.7}N_{0.3}$, $TiC_{0.5}N_{0.5}$ and $TiC_{0.3}N_{0.7}$ exhibit a sharp decrease in the CO production at the temperature of liquid phase formation (arrows in Fig. 6a-c). This temperature increases with decreasing carbon content in the carbonitride. Below the temperature of the formation of the liquid phase there is an intensive interaction between hard particles and binder metal, resulting in solid state sintering. Dilatometric measurements show that the densification of the sintered bodies starts at temperatures of more than 200°C below the formation of liquid phase by solid state sintering (Fig. 7). The mobility of carbon is increased in this temperature region and therefore the remain-

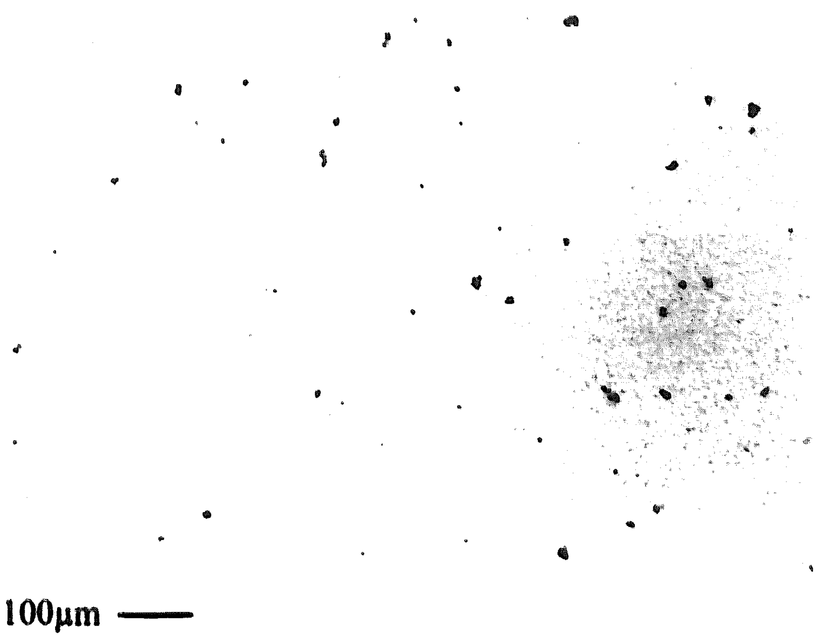

Fig. 5. Microstructure of a Fe–TiC composite, heated up to 1550°C at 25 K/min.

ing surface oxides can be removed. If the oxygen content in the hard particles is low, this reaction is completed when the binder is molten. If the binder contains too much oxygen, the hard particles are oxidised to a greater extent during the solid-state sintering and the decrease in the CO production curve is less pronounced. The nitrogen outgasing of the samples increases with the nitrogen content of the carbonitride. The CO peak at 1230°C in the Fe–$TiC_{0.7}N_{0.3}$ sample is caused by an internal reduction of the carbonitride, the pure carbonitride also releases CO at this temperature. The Fe–TiN sample shows a nitrogen release beginning at approximately 1300°C caused by an oxidation of the nitride by oxygen from the iron powder. Thus, Ti(O,N) is formed in accordance with the work of Khrustalev [7]. At higher temperatures, the dissolution of titanium in the binder phase and parallel nitrogen removal take place also.

The shrinkage of Fe–TiC_xN_{1-x} samples during liquid phase sintering increases with decreasing nitrogen content, as shown in Fig. 8. This is due to the higher carbon activity in carbon-rich carbonitrides which allows a more easy reduction of the surface oxides on the hard particles and an increased carbon diffusion into the binder, resulting in a lower melting point.

4. Conclusions

The reaction behaviour during sintering can be divided into three sections. At low temperatures (up to 500°C) physical reactions take place, in particular the vaporisation of residual milling agent and desorption of CO from the metal phase. In the medium temperature range, beginning at approximately 500°C and extending up to the melting point of the binder metal, the reduction of surface oxides takes place. The CO evaluation increases at temperatures below the formation of the liquid phase. Obviously two phenomena occur which increase the wettability of carbides by Fe:

1. Carbon diffusion out of the carbide into the binder
2. Oxygen removal by CO formation

A small oxygen content at the surface of the hard particles can be removed in the solid state under vacuum and improves the wettability. Higher oxygen contents (> 0.4 wt.% total oxygen) is harmful, because it decreases the wettability by the liquid binder and the removal leads to increased CO liberation, both of which favour pore formation, resulting in poor quality of the sintered bodies. The extent of pore formation can be reduced by a slight increase of the pressure in the presence of the liquid phase.

In the third region, starting at the temperature of formation of the liquid phase, the liquid binder starts to dissolve the hard particles beginning at the grain boundaries. When the binder is saturated a solution–dissolution reaction takes place, reshaping and increasing the size of the hard particles.

The densification of Fe–$Ti(C_xN_{1-x})$ cermets during the sintering is dependent on the carbon content in the carbonitride, due to carbon diffusion in the binder.

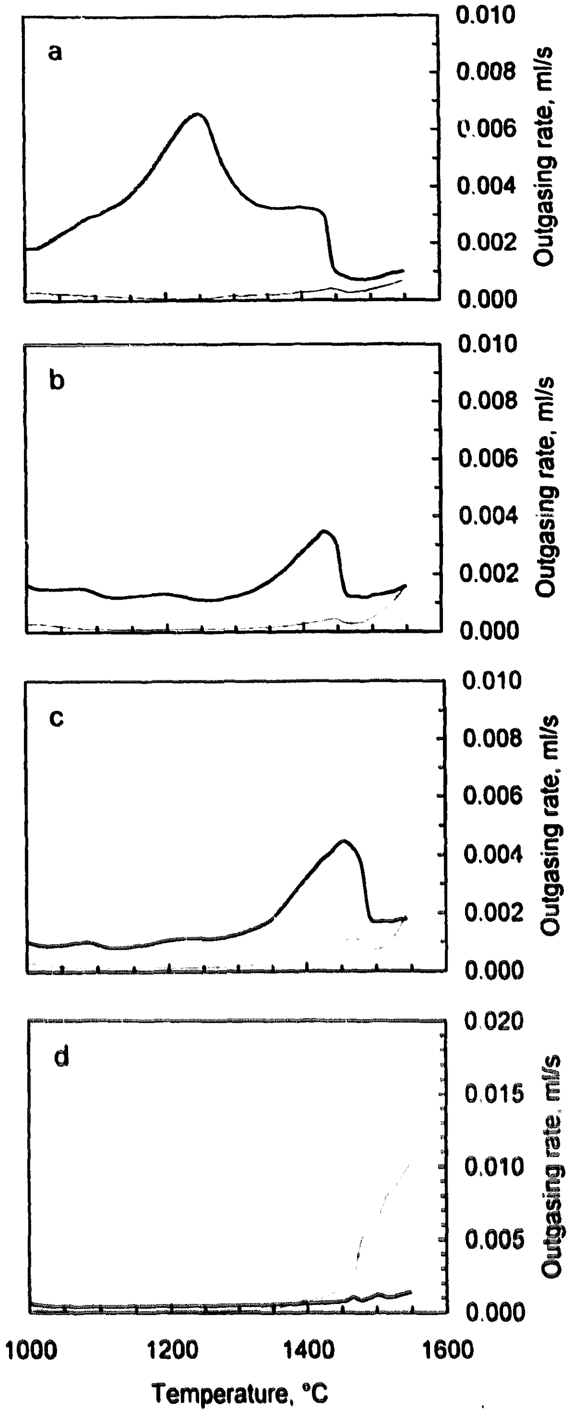

Fig. 6. Outgasing behaviour of Fe–TiC$_x$N$_{1-x}$ composites (a: Fe–TiC$_{0.7}$N$_{0.3}$; b: Fe–TiC$_{0.5}$N$_{0.5}$; c: Fe–TiC$_{0.3}$N$_{0.7}$; d: Fe–TiN), thick line represents CO and the thin line represents N$_2$ formation.

Acknowledgement

This work was supported by the 'Jubiläumsfonds der Oesterreichischen Nationalbank' under project No. 4876

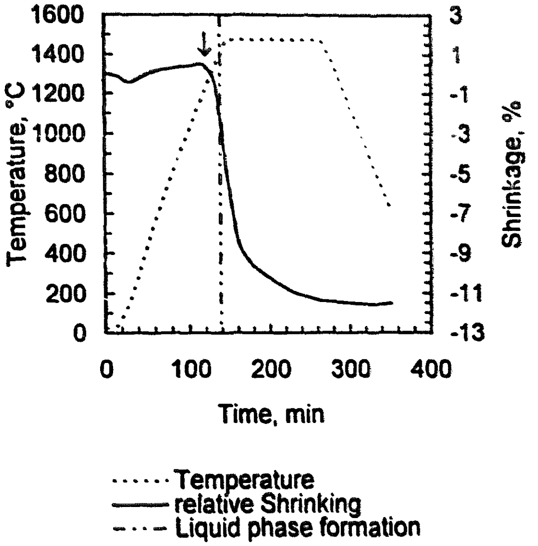

Fig. 7. Dilatometric measurement of a Fe–TiC$_{0.7}$N$_{0.3}$ composite, heated at a rate of 10 K/min up to 1475°C and held for 2 h. The shrinking starts more than 200°C below the formation of the liquid phase.

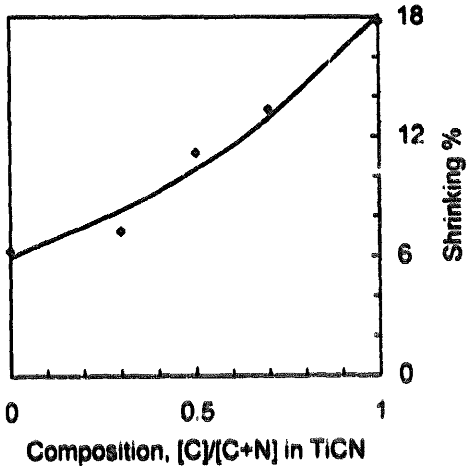

Fig. 8. Shrinking during sintering Fe–TiC$_x$N$_{1-x}$ composites up to 1550°C at a rate of 25 K/min as a function of the [C]/[C + N] ratio in the hard phase.

References

[1] A. Maurer, J. Hard Mater. 3/3 (1992) 235.
[2] R.F. Bunshah, Trans. Natl. Vac. Symp. 98 (1966) 98.
[3] V. Popov, Fiz. Met. Metalloved. 76/5 (1994) 156.
[4] Y. Murakami, et al., Nippon Kinzoku Gakkaishi 21 (1957) 712.
[5] W. Tofaute, et al., Arch. Eisenhüttenwes. 12 (1938) 33.
[6] A.K. Shurin, G.P. Dmitrieva, Metalloved. Term. Obrab. Met. 8 (1974) 27.
[7] B. Khrustalev, B. Leonovich, Tr. Chelyab. Politekh. Inst. 133 (1974) 42.